

LETTERS

A Direct Observation of Non-RRKM Behavior in Femtosecond Photophysically Activated Reactions**I-Ren Lee, Wei-Kan Chen, Yu-Chieh Chung, and Po-Yuan Cheng****Department of Chemistry, National Tsing Hua University, Hsinchu, Taiwan 30043, R.O.C.**Received: August 24, 2000; In Final Form: October 2, 2000*

A nonstatistical behavior has been observed in the photodissociation of two acyl cyanide compounds, R-C(O)-CN, where R = methyl and *tert*-butyl groups. The initial activation was achieved by femtosecond two-photon excitation followed by ultrafast internal conversion. The excited-state dissociation dynamics was followed in real time by monitoring the temporal evolution of CN (X) products. The observed product appearance time constants are in picosecond time scales and are markedly similar for the two compounds studied. Our analyses revealed that the excited-state dissociation rate does not decrease with molecular size as much as statistical rate theory predicts, suggesting a nonergodic system in which the available vibrational energy does not redistributed statistically among all modes before the bond breakage occurs.

The central assumptions in the Rice–Ramsperger–Kassel–Marcus (RRKM) theory are that the intramolecular vibrational energy redistribution (IVR) is much faster than the reaction and that the phase space density is uniform during the entire course of the reaction.^{1–4} The satisfactory agreements generally found between the RRKM theory and many different types of experiments have made it one of the most important models in predicting unimolecular reaction rates today.^{2–5} However, there has been experimental evidence revealing that the basic assumptions of RRKM theory are not always valid.^{6–12} Bunker and Hase¹³ had recognized that the deviation can occur because of a “bottleneck” in the phase space (intrinsic non-RRKM) or because of a time scale for reaction which prevents the statistical redistribution of internal energy prior to the reactions (apparent non-RRKM). To observe the initial apparent non-RRKM behavior, one has to be able to prepare a nonrandom initial distribution in the reactant phase space and monitor the reaction at short times. The early experiments of Rabinovitch and co-workers^{6,7} used chemical activation to prepare reacting molecules with nonrandom distribution among all internal modes,

and they observed the apparent non-RRKM behavior by using collisional quenching as a clock. The recent experiments reported by Zewail’s group^{11,12} employed femtosecond activation to define a nonrandom distribution in the reactant phase space on a time scale much faster than the IVR and reactions. The activation was achieved via an ultrafast bond breaking induced by femtosecond laser excitation. They observed clear apparent non-RRKM behavior even though the total energy was nearly 100 kcal/mol above the reaction barrier!¹²

In this letter, we report on our recent observations of apparent non-RRKM behavior in the photodissociation of acetyl cyanide and pivaloyl cyanide (see Figure 1). The two compounds are different only in the size of their alkyl substituents. The initial preparation was achieved by femtosecond Franck–Condon optical pumping followed by an ultrafast internal conversion process. Both compounds were excited through a two-photon transition at ~ 388 nm to the ~ 6.4 eV energy region. A second delayed pulse, also at ~ 388 nm, then probed the temporal evolution of the free CN (X) fragments by monitoring the CN X \rightarrow B laser-induced fluorescence (LIF) signal. The laser pulses were generated from a regeneratively amplified Ti:sapphire

* Corresponding author. E-mail: pycheng@mx.nthu.edu.tw.

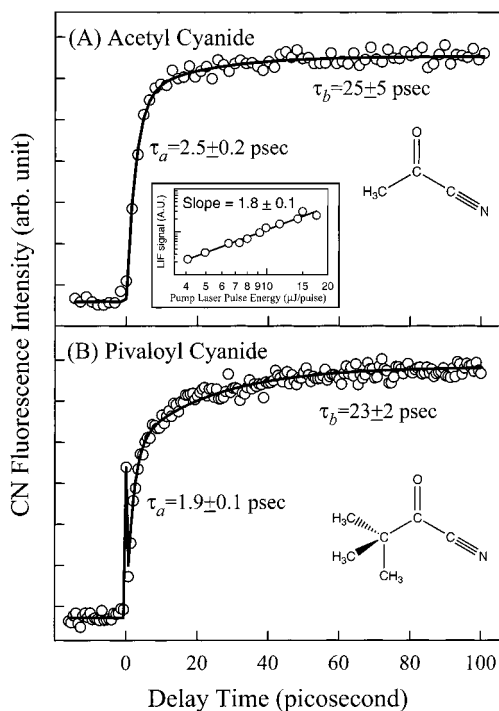


Figure 1. Transients observed by monitoring the CN $X \rightarrow B$ LIF signal as a function of the pump-probe delay time for the photodissociation of acetyl cyanide (A) and pivaloyl cyanide (B) upon two-photon excitation at ~ 388 nm. The time constants were obtained by simultaneously fitting short-time (not shown) and long-time scale transients to biexponential rise functions. The open circles are the experimental data points, and the solid lines are the best fits. The inset in (A) shows the pump laser intensity dependence of the LIF signal with the data plotted on a log-log scale. The slope of ~ 1.8 of the best-fitted straight line indicates a two-photon process. The spiking feature in the (B) transient is due partly to the enhanced multiphoton absorption occurring at the zero delay time. The higher yield of CN (X) in the acetyl cyanide case allowed us to use lower laser pulse energies, resulting in a much weaker initial spike that is invisible at the large time intervals used here. Note that in both cases, the laser-intensity-dependence studies have indicated that the subsequent rises are due to two-photon absorption of the pump and that their shapes do not change upon further reduction in the pump pulse energy by a factor of 2–3.

mode-locked femtosecond laser system operating at a repetition rate of 1 kHz. The amplifier output was split and frequency doubled to produce the pump and probe pulses at 388 nm with a cross-correlation of about 200 fs (fwhm). Neutral density filters were used to adjust the pulse energies of both beams to ~ 5 – 20 μ J for the pump and ~ 0.5 – 1.0 μ J for the probe. Typically, the pulse energy of the pump was about 10–20 times greater than that of the probe, making the negative-time signal negligible in comparison with the positive-time signal. The two beams were collinearly recombined via a beamsplitter and focused into a gas flow cell through a $f = 50$ cm lens. The transients were obtained by monitoring the fluorescence signal as a function of the pump-probe delay time.

Figure 1 shows the observed temporal evolution of CN (X) products for both compounds. Since it is not energetically possible for one 388 nm photon to eliminate CN from these two compounds, the observed signal must be a result of two- or more photon excitation. We have performed careful laser intensity (see inset in Figure 1) and wavelength dependence studies to ensure that the LIF signal arises from CN (X) fragments produced upon two-photon excitation of the two compounds at 388 nm. As shown in Figure 1, both transients can be well characterized by biexponential rise functions. The rise time constants obtained from the nonlinear least-squares

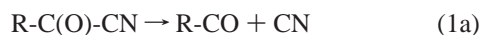
fitting are $\tau_a = 2.5 \pm 0.2$ ps and $\tau_b = 25 \pm 5$ ps for acetyl cyanide and $\tau_a = 1.9 \pm 0.1$ ps and $\tau_b = 23.0 \pm 0.5$ ps for pivaloyl cyanide. The amplitude ratio of the two components (A_a/A_b) decreases from 4.5 ± 0.5 for acetyl cyanide to 2.0 ± 0.1 for pivaloyl cyanide, as manifested in the more pronounced biexponential appearance of the pivaloyl cyanide transient. These time-resolved data provide important implications to the dissociation dynamics occurring in acyl cyanides. Indeed, the observed picosecond time scales immediately indicate that the initial excitation to the near 6.4 eV energy region does not access a repulsive surface directly and the dissociation proceeds via a complex-mode mechanism.

One striking feature of our results is the essentially identical reaction times observed for both compounds. Since there is a large difference in the numbers of vibrational modes between these two compounds (18 for acetyl cyanide and 45 for pivaloyl cyanide) and since the dissociation proceeds via a complex-mode mechanism, statistical rate theory would predict that pivaloyl cyanide dissociates much slower than acetyl cyanide does.^{2–4} Although the nearly identical rise times could imply that the reactions are nonstatistical, one has to be cautious here because other decay channels can compete efficiently with the dissociation and dominate the rise times. Detailed dissociation pathways need to be elucidated first. In the following discussion, we will first briefly review some previous results relevant to the present work. We then describe a proposed mechanism to show that even when other excited-state decay channels are taken into account, the non-RRKM behavior still persists.

The absorption spectra of acetyl cyanide in the vapor phase have been reported previously.^{14–17} The first absorption band is weak and centers at ~ 310 nm. It has been attributed to the characteristic $n_{\text{O}} \rightarrow \pi^*_{\text{CO}}$ transition of carbonyl compounds. Yoon et al.¹⁷ have investigated this band in free jets in some detail and have determined its origin at $27\,511$ cm^{-1} . The onset of the next absorption band, which is also very weak, occurs at ~ 225 nm.¹⁶ This weak band is then followed by a series of strong absorption bands beginning at ~ 200 nm.¹⁶ The state excited near 6.4 eV (193 nm) has been tentatively assigned to the $^1(n_{\text{O}}, 3s)$ Rydberg state,^{14,18} in analogy with the absorption of acetone in the similar energy region. Recently, Owrutsky and Baronavski argued that the absorption at 193 nm is due to the $\pi_{\text{CN}} \rightarrow \pi^*_{\text{CO}}$ transition on the basis of their ab initio calculations using the time dependent density functional formalism.¹⁶ The energy of the corresponding state was calculated to be 6.28 eV, consistent with the experimental value of 6.20 eV for the onset of the third absorption band. In the simple molecular-orbital picture, this transition involves the promotion of an electron from the out-of-plane π orbital on the CN moiety to the π^* orbital localized on the CO moiety. The excitation is thus essentially localized along the $\text{O}=\text{C}-\text{C}\equiv\text{N}$ backbone. In the following discussion, we denote the initial state excited near the 6.4 eV energy region as S_3 , since there are two other lower singlet excited states that have been identified.^{16,17} We took the observed onsets of the second and third absorption bands¹⁶ as the zero points for the S_2 and S_3 states, respectively. Owrutsky and Baronavski also studied the photodissociation of acetyl cyanide at 193 nm using femtosecond mass-resolved multiphoton ionization spectroscopy.¹⁶ They observed a pulse width limited decay (< 200 fs) by monitoring the parent mass channel. However, in view of our observations of picosecond product rises, the ultrafast parent decay should be interpreted as the initial-state decay and does not reflect the time needed for the excited molecules to fall apart.

The photodissociation of acetyl cyanide has been studied by

several groups, with special emphasis on the bond-selective chemistry.^{14,15,18} Recently, Furlan et al.¹⁵ investigated the photodissociation of a series of acyl cyanides, R-C(O)-CN, where R = methyl, isopropyl, and *tert*-butyl, at 193 nm (6.4 eV) using photofragment translation spectroscopy. They found that the dominant decay processes are the primary dissociation of the two nonequivalent α -C-C bonds



The bond dissociation energies of the two α -bonds in acetyl cyanide (R = CH₃) have been predicted to be $D_0(\text{C-CN}) = 427$ kJ/mol and $D_0(\text{C-CH}_3) = 359$ kJ/mol on the bases of the results of ab initio calculations and available thermochemical data.¹⁸ The stronger C-CN bond clearly suggests a partial conjugation between the CO and CN moieties. If sufficient energy is partitioned into the internal degrees of freedom of the primary photofragments, secondary dissociation can subsequently occur



Nevertheless, they found that the secondary dissociation (eq 2b) is unimportant ($\leq 5\%$) for all the compounds studied, suggesting that nearly all CN fragments arise from the primary CN elimination (eq 1a).¹⁵ Furthermore, no evidence of molecular elimination channels has been observed. In the case of acetyl cyanide, they concluded that the CN elimination reaction is the dominant channel with a total branching of $85 \pm 10\%$, whereas the CH₃ elimination channel occurs with a branching of only $15 \pm 10\%$.¹⁵ Clearly, there is a strong preference for the primary CN elimination reaction (eq 1a) over the CH₃ elimination reaction (eq 2a) in the photodissociation of acetyl cyanide despite the stronger α -C-CN bond. Interestingly, this preference exists only in acetyl cyanide. The branching for the CN elimination decreases to $30 \pm 10\%$ for isobutyryl cyanide (R = isopropyl) and $17 \pm 10\%$ for pivaloyl cyanide (R = *tert*-butyl). On the basis of the product translational energy distributions, they suggested that the formation of electronically excited CN and/or acetyl radicals might be responsible for the preferred C-CN bond breaking in acetyl cyanide.¹⁵

We have proposed a mechanism, which will be detailed in a forthcoming full account of this work,¹⁹ for the photodissociation of acetyl cyanide (and other similar acyl cyanides) based on the available experimental results and theoretical considerations of the acetyl cyanide excited states and their correlation with the energetically accessible product states. The proposed mechanism and the cuts through the potential energy surfaces of relevant states along the two dissociation coordinates are schematically illustrated in Figure 2. The femtosecond two-photon excitation at 388 nm initially prepares a wave packet on the S₃ surface, followed by an ultrafast internal conversion process (IC1) to the S₂ state in ~ 100 fs. The evidence for this ultrafast internal conversion comes from our observation of a time delay of about 100 fs in the product rise, revealed in short-time scale transients (not shown) with smaller step sizes,¹⁹ and the ultrafast parent decay observed by Owrutsky and Baronavski¹⁶ in their time-resolved multiphoton ionization experiments. Following the internal conversion, the system quickly moves on the S₂ surface and dissociates adiabatically (D1) to form "CN(X) + R-CO(\tilde{A})" via a barrier.²⁰ The adiabatic dissociation channel (D1) on the S₂ surface is responsible for producing the ground-state CN detected in the fast component

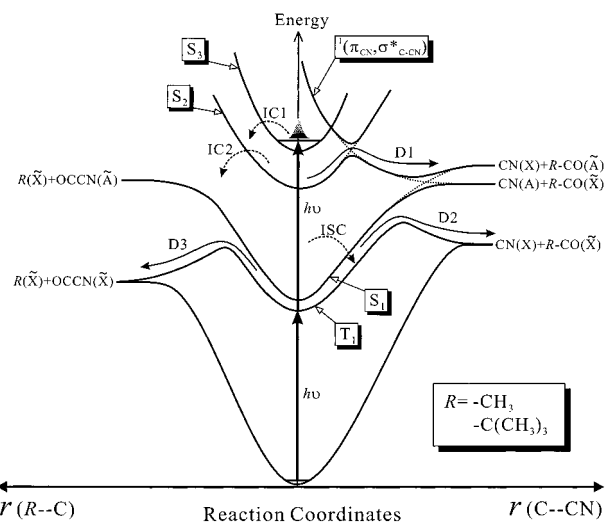


Figure 2. Schematic diagram showing cuts through the potential energy surfaces of relevant states along the C-CN and R-C dissociation coordinates for the two acyl cyanide compounds discussed here. The energetics of the minima and asymptotes are drawn to scale according to the best-known literature values for acetyl cyanide.¹⁵⁻¹⁸ The proposed mechanism is also illustrated in the diagram using curved arrows. Note that the solid arrows represent adiabatic processes occurring along the two coordinates specifically indicated by the directions of the arrows, whereas the dashed arrows represent processes that do not necessarily occur along the two coordinates. The locations and directions of these dashed arrows shown in the diagram are somewhat arbitrary.

of the transients shown in Figure 1. Note that the S₂ surface correlates adiabatically along the R-C dissociation coordinate to products that are energetically inaccessible in our experiments. While moving on the S₂ surface, some trajectories can lead to the lower S₁ surface via nonadiabatic coupling (IC2) to S₁, which is then followed by fast intersystem crossing (ISC) to the lowest triplet state T₁. Once on the T₁ surface, the system can exit adiabatically to either "CN(X) + R-CO(\tilde{X})" (D2) or "R(\tilde{X}) + OCCN(\tilde{X})" (D3) over corresponding barriers.²¹ The CN(X) fragments produced in the C-CN cleavage (D2) on the T₁ surface give rise to the observed slower components. Overall, the rise time for the faster component is determined by the sum of the rates of all S₂ decay channels, whereas the rise time for the slower component is governed by the rates of the S₁ → T₁ ISC and the two adiabatic dissociation steps on the T₁ surface. Since the dissociation on the T₁ surface at this high energy is likely to be on the subpicosecond time scales, we speculate that the S₁ → T₁ ISC is the rate-determining step for the slower component. This mechanism is fully consistent with our observations as well as with the results reported by Furlan et al.,¹⁵ who also concluded that a major portion of the C-CN primary dissociation leads to electronically excited products in the photodissociation of acetyl cyanide. The loss of preference for the CN elimination in pivaloyl cyanide¹⁵ is simply due to its slower adiabatic dissociation on the S₂ surface (see below) and faster internal conversion to S₁.

On the basis of this proposed mechanism, we determined²² the time constants ($1/k_{D1}$) for adiabatic dissociation on the S₂ surface to be 3.6 ps for acetyl cyanide and 16.8 ps for pivaloyl cyanide using our time-resolved data and the branching reported by Furlan et al.¹⁵ for the primary CN and alkyl elimination channels. These are the adiabatic dissociation time constants on the S₂ surface if there were no other decay channels present. Thus, the presence of the large *tert*-butyl group does slow down

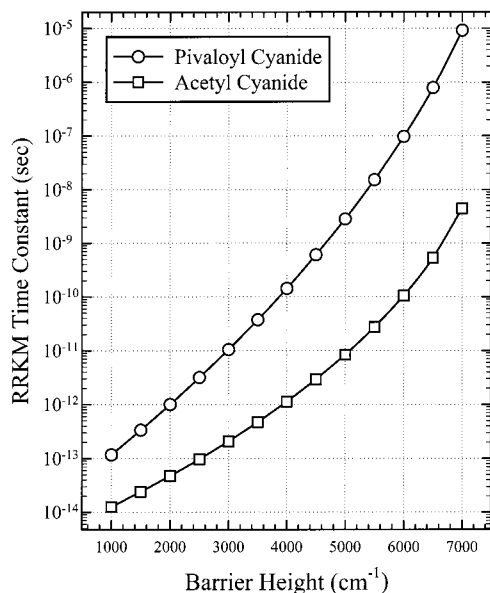


Figure 3. RRKM time constants ($1/k_{\text{RRKM}}$) for the CN elimination reactions of acetyl cyanide and pivaloyl cyanide on their S_2 surfaces as a function of barrier heights in the range from 1000 to 7000 cm^{-1} . The rates were calculated with the procedures described in the text. Note that the time constants are plotted on a logarithm scale.

the adiabatic dissociation on the S_2 surface by a factor of about 5, which is still much less than expected on the basis of statistical rate theory.

To elucidate the nonstatistical nature of the dissociation, we carried out RRKM calculations using the expression^{3,4}

$$k_{\text{RRKM}}(E) = \frac{N^\ddagger(E - E_0)}{h\rho(E)}$$

where E is the available internal energy in S_2 , E_0 is the C–CN dissociation barrier height on the S_2 surface with zero-point energy correction, N^\ddagger is the number of energetically accessible states at the transition state, and ρ is the density of the reactant states. The vibrational frequencies of the lowest triplet state (T_1) obtained from ab initio calculations were used as an approximation for the S_2 state frequencies needed in the RRKM calculations. The structures of the T_1 state minimum and its C–CN dissociation transition state were optimized at the unrestricted B3LYP/6-31G(d) level of theory using the Gaussian94 program²³ for both compounds. The method of intrinsic reaction coordinate (IRC) was used to confirm that the calculated transition states lead to CN elimination.²⁴ The harmonic vibrational frequencies were then calculated at the same level of theory. The calculated vibrational frequencies of the acetyl cyanide T_1 state were found to be consistent with the experimental values reported for its S_0 and S_1 states.^{17,18} The density of states (ρ) and the number of states (N^\ddagger) were then calculated using the Beyer–Swinehart direct state-counting algorithm for harmonic oscillators.²⁵ The available internal energy (E) in the S_2 state is about 7700 cm^{-1} for acetyl cyanide and about 8300 cm^{-1} for pivaloyl cyanide.²⁶ The barrier height (E_0) on the S_2 surface is unknown, and it is difficult to obtain a reliable prediction by electronic structure calculations. We therefore calculated the RRKM rates for barrier heights within a reasonable range of 1000–7000 cm^{-1} , as shown in Figure 3. It has been reported that for a number of alkyl methyl ketones, R–C(O)–CH₃, the barrier heights for the α -cleavage of the CH₃ group are independent of the nature of R and are nearly the same for R = methyl and *tert*-butyl groups.²⁷ Accordingly, we

expect the barrier heights for CN elimination to be similar for acetyl cyanide and pivaloyl cyanide.

As shown in Figure 3, the calculated rate strongly depends on the barrier height and is slower for pivaloyl cyanide, as expected. With a barrier height of $\sim 4500 \text{ cm}^{-1}$ on the S_2 surface, the RRKM rate agrees with the experimental value for acetyl cyanide. Nevertheless, with the same barrier height, the theory predicted that pivaloyl cyanide dissociates at a rate about 200 times slower than acetyl cyanide does, yet the experimental results showed only a factor of 5 slower! The ratio of the RRKM rates of the two compounds (acetyl cyanide/pivaloyl cyanide) increases with the barrier height, reaching more than 3 orders of magnitude at $E_0 = 7000 \text{ cm}^{-1}$. On the other hand, the ratios become close to the experimental value for very low barriers ($\sim 1000 \text{ cm}^{-1}$) with predicted time constants in the 10–100 fs time scales. As will be discussed below, the nature of the electronic transitions involved in the initial preparation implies an initial phase space distribution near the reaction exit, making the RRKM rates lower than the observed values. Consequently, the barrier height is more likely to be greater than 4500 cm^{-1} . The RRKM theory thus predicts a decrease in dissociation rates by more than 2 orders of magnitude on going from methyl to *tert*-butyl substitution in these two acyl cyanides. Clearly, our experimental results reveal a strong deviation from the RRKM predictions.

The reason for this non-RRKM behavior is probably due to the nonuniform initial phase space distribution and the slow IVR. Since the initial excitation reaches the S_3 ($\pi_{\text{CN}}, \pi^*_{\text{CO}}$) state involving mainly the CN and CO conjugated moieties, the equilibrium geometries of S_3 and S_0 are expected to be quite different along the O=C–C \equiv N backbone. Consequently, femto-second excitation to the Franck–Condon region in S_3 would prepare an initial wave packet with its vibrational energy concentrated along the O=C–C \equiv N backbone. The subsequent ultrafast internal conversion in ~ 100 fs would also deposit a significant fraction of vibrational energy along the O=C–C \equiv N backbone in S_2 . On the other hand, the CH₃–C moiety in acetyl cyanide and the (CH₃)₃–C moiety in pivaloyl cyanide are much less perturbed during the initial optical excitation and the subsequent internal conversion because of their similar local geometries in the relevant states. Thus, the initial femtosecond photophysical preparation produces a relatively “hot” O=C–C \equiv N backbone and a relatively “cold” alkyl group in ~ 100 fs. It is plausible that the non-RRKM behavior observed here is simply due to the inefficient coupling between the vibrational modes of these two moieties, making the flow of vibrational energy from the O=C–C \equiv N backbone to the alkyl groups slower than the reactions. In other words, the initial activation prepares a phase space distribution more concentrated in a region closer to the reaction exit. The poor coupling between the initially more populated region and the other regions restricts IVR to certain modes near the reaction coordinate and prevents the system from sampling the entire phase space in the reaction time scale of ~ 2 ps.

The vibrational state density in S_2 at the available internal energy is $\sim 4.46 \times 10^4/\text{cm}^{-1}$ for acetyl cyanide and $\sim 3.11 \times 10^{10}/\text{cm}^{-1}$ for pivaloyl cyanide, i.e., an increase by more than 5 orders of magnitude. Our results suggest that a great portion of this level-density increase arises from modes that are not coupled to the initially excited modes and that the IVR rates do not change in proportion to the density of states. Similar behaviors have been observed in studies of IVR dynamics using frequency-resolved techniques.^{28,29} For example, in studies of a series of compounds (CX₃)₃C–C \equiv CH,^{30–32} where X =

H, D, and F, the spectral line width measurements revealed that the IVR rates for the singly excited acetylenic C–H stretch ($\nu_{\text{CH}} = 1$) change only by a factor of 5 even though the vibrational state densities span over 4 orders of magnitude for these three compounds.

In conclusion, we have observed an apparent non-RRKM behavior in the femtosecond photophysically activated dissociation of acetyl cyanide and pivaloyl cyanide. The method takes the advantage of the ultrafast internal conversion (~ 100 fs) occurring in a high-lying electronic state to define a vibrational excitation temporally and spatially in a lower state. We proposed that inefficient coupling between the initially more excited O=C–C \equiv N moiety and the alkyl-group prevent the system from redistributing vibrational energy statistically through the phase space before reaction occurs. The dynamical picture revealed here can be related to the model described recently by Remacle and Levine³³ for the prompt dissociation of energy-rich large molecules, since the energy is initially “localized” near the transition-state region. The present results also imply the possibility for bond-selective chemistry in large molecules having poor coupling between different parts of molecules, even if the reactions are in picosecond time scales!

Acknowledgment. This work was supported by a grant from the National Science Council (NSC89-2113-M-007-014) of the Republic of China.

References and Notes

- Marcus, R. A. *J. Chem. Phys.* **1952**, *20*, 359.
- Frost, W. *Theory of Unimolecular Reactions*; Academic Press: New York, 1973.
- Gilbert, R. G.; Smith, S. C. *Theory of Unimolecular and Recombination Reactions*; Blackwell: London, 1990.
- Baer, T.; Hase, W. L. *Unimolecular Reaction Dynamics: Theory and Experiments*; Oxford: New York, 1996.
- Hase, W. L. *Acc. Chem. Res.* **1998**, *31*, 659.
- Oref, I.; Rabinovitch, B. S. *Acc. Chem. Res.* **1979**, *12*, 166 and references therein.
- Flowers, M. C.; Rabinovitch, B. S. *J. Phys. Chem.* **1985**, *89*, 563.
- Osterheld, T. H.; Brauman, J. I. *J. Am. Chem. Soc.* **1993**, *115*, 10311.
- Semmes, D. H.; Baskin, J. S.; Zewail, A. H. *J. Am. Chem. Soc.* **1987**, *109*, 4104.
- Semmes, D. H.; Baskin, J. S.; Zewail, A. H. *J. Chem. Phys.* **1990**, *92*, 3359.
- Kim, S. K.; Guo, J.; Baskin, J. S.; Zewail, A. H. *J. Phys. Chem.* **1996**, *100*, 9202.
- Diau, E. W. G.; Herek, J. L.; Kim, Z. H.; Zewail, A. H. *Science* **1998**, *279*, 847.
- Bunker, D. L.; Hase, W. L. *J. Chem. Phys.* **1973**, *59*, 4621.
- North, S. W.; Marr, A. J.; Furlan, A.; Hall, G. E. *J. Phys. Chem. A* **1997**, *101*, 9224.
- Furlan, A.; Scheld, H. A.; Huber, J. R. *J. Phys. Chem. A* **2000**, *104*, 1920.
- Owrustsky, J. C.; Baronavski, A. P. *J. Chem. Phys.* **1999**, *111*, 7329.
- Yoon, M.-C.; Choi, Y. S.; Kim, S. K. *J. Chem. Phys.* **1999**, *110*, 7185.
- Horwitz, R. J.; Francisco, J. S.; Guest, J. A. *J. Phys. Chem. A* **1997**, *101*, 1231.
- Lee, I. R.; Chung, Y. C.; Chen, W. K.; Hong, X. P.; Cheng, P. Y. *J. Chem. Phys.*, manuscript in preparation.
- The barrier is formed by an avoided crossing between the dominant electronic configuration of S_2 at the Franck–Condon region, $^1(a''\pi_{\text{CN}}, \pi^*_{\text{CO}})$, and the $^1(a''\pi_{\text{CN}}, \sigma^*_{\text{C-CN}})$ repulsive configuration. The latter interacts again with the $^1(n_{\text{O}}, \pi^*_{\text{CO}})$ configuration to form the adiabatic pathway leading to “CN(X) + R-CO($\dot{\text{A}}$)” products.
- The barriers on the T_1 surface arise from interactions between the dominant electronic configuration of T_1 at the Franck–Condon region, $^3(n_{\text{O}}, \pi^*_{\text{CO}})$, and the purely repulsive configurations $^3(\sigma, \sigma^*)_{\text{C-CN}}$ and $^3(\sigma, \sigma^*)_{\text{CH}_3-\text{C}}$ along the two dissociation coordinates. Strictly speaking, they form conical intersections, and the crossings are avoided only when the plane of symmetry is distorted. Our ab initio calculations at the UB3LYP/6-31G(d) level of theory indeed showed that both transition states are nonplanar.
- The amplitude ratio of the fast to slow components observed in our experiments reflects the yield ratio between the D1 and D2 channels (D1/D2), which is $\sim 4.5/1$ for acetyl cyanide and $\sim 2.0/1$ for pivaloyl cyanide. On the other hand, the results from Furlan et al.¹⁵ suggested that (D1 + D2)/D3 $\approx 85/15$ and $17/83$ for acetyl cyanide and pivaloyl cyanide, respectively, on the basis of our mechanism. From these, one can obtain the branching ratio for the competing reactions of D1 and IC2, which is equivalent to $k_{\text{D1}}/k_{\text{IC2}}$. Combined with the relation of $k_{\text{D1}} + k_{\text{IC2}} = 1/\tau_a$, where τ_a is the measured time constant for the fast component, the rate constant for the D1 step can be determined.
- Frisch, M. J.; Trucks, G. W.; Schlegel, H. B.; Gill, P. M. W.; Johnson, B. G.; Robb, M. A.; Cheeseman, J. R.; Keith, T.; Petersson, G. A.; Montgomery, J. A.; Raghavachari, K.; Al-Laham, M. A.; Zakrzewski, V. G.; Ortiz, J. V.; Foresman, J. B.; Cioslowski, J.; Stefanov, B. B.; Nanayakkara, A.; Challacombe, M.; Peng, C. Y.; Ayala, P. Y.; Chen, W.; Wong, M. W.; Andres, J. L.; Replogle, E. S.; Gomperts, R.; Martin, R. L.; Fox, D. J.; Binkley, J. S.; Defrees, D. J.; Baker, J.; Stewart, J. P.; Head-Gordon, M.; Gonzalez, C.; Pople, J. A. *Gaussian 94*, Revision E. 3; Gaussian, Inc.: Pittsburgh, PA, 1995.
- Gonzalez, C.; Schlegel, H. B. *J. Chem. Phys.* **1989**, *90*, 2154; *J. Phys. Chem.* **1990**, *94*, 5523.
- Beyer, T.; Swinehart, D. R. *Commun. Assoc. Comput. Machin.* **1973**, *16*, 379.
- The available internal energy in S_2 was calculated with $E_{\text{int}} = E_{\text{hv}} + E_{\text{therm}} - E_0$, where E_{hv} is the total two-photon excitation energy, E_{therm} is the average thermal vibrational energy at 298 K, and E_0 is the energy of the $S_2 \leftarrow S_0$ transition origin. We took the onset of the acetyl cyanide second absorption band at 5.51 eV¹⁶ as the $S_2 \leftarrow S_0$ transition origin for both compounds, since their absorption spectra are nearly identical in terms of band positions.¹⁵ E_{therm} was estimated by ab initio electronic structure calculations.
- Reinsch, M.; Klessinger, M. *J. Phys. Org. Chem.* **1990**, *3*, 81.
- Lehmann, K. K.; Scoles, G.; Pate, B. H. *Annu. Rev. Phys. Chem.* **1994**, *45*, 241 and references therein.
- Nesbitt, D. J.; Field, R. W. *J. Phys. Chem.* **1996**, *100*, 12735 and references therein.
- Kerstel, E. R. Th.; Lehmann, K. K.; Mentel, T. F.; Pate, B. H.; Scoles, G. *J. Phys. Chem.* **1991**, *95*, 8282.
- Gambogi, J. E.; L'Esperance, R. P.; Lehmann, K. K.; Pate, B. H.; Scoles, G. *J. Chem. Phys.* **1993**, *98*, 1112.
- Gambogi, J. E.; Lehmann, K. K.; Pate, B. H.; Scoles, G.; Yang, X. *J. Chem. Phys.* **1993**, *98*, 1748.
- Remacle, F.; Levine, R. D. *J. Phys. Chem. A* **1998**, *102*, 10195.